Vacuum 203 (2022) 111240

Contents lists available at ScienceDirect

Vacuum

journal homepage: www.elsevier.com/locate/vacuum

Linear Energy Transfer (LET) dependence of graphene oxide dosimeter for different ionizing radiations

L. Torrisi [a,e,*], L. Silipigni [a,e], M. Cutroneo [b,e], E. Proverbio [c], A. Torrisi [d,f]

[a] Dip.to di Scienze Fisiche, MIFT, Università di Messina, V.le F.S. D'Alcontres 31, 98166, Messina, Italy
[b] Nuclear Physics Institute of the CAS, Hlavní 130, 250 68, Husinec Řež, Czech Republic
[c] Dip.to Ingegneria, Università di Messina, C.da Di Dio, 98166, Messina, Italy
[d] Dipartimento di Fisica di Lecce e INFN Sezione di Lecce, V. per Arnesano, 73100, Lecce, Italy
[e] INFN-Sezione di Catania, Viale A. Doria 44, 95123, Catania, Italy
[f] INFN-Sezione di Lecce, V. per Arnesano, 73100, Lecce, Italy

ARTICLE INFO

Keywords:
Graphene oxide dosimetry
Linear energy transfer (LET)
XPS spectroscopy
EDX analysis
Raman spectroscopy

ABSTRACT

The graphene oxide (GO) reduction by ionizing radiation is proportional to the absorbed dose due to the energy release which produces ionizations, deexcitations, chemical bonding breaking, radical formation and recombination, oxygen functional groups and water desorption. Thanks to this, GO can be employed as a dosimeter whose dose can be measured using different analysis techniques, such as Raman spectroscopy, X-ray diffraction (XRD) and Energy Dispersive X-ray (EDX) analysis based on the characteristic X-ray emission, X-ray photoelectron spectroscopy (XPS). To evaluate the GO reduction as a function of the Linear Energy Transfer (LET) of the used radiation, measurements have been performed with XPS and EDX to deduce the C/O atomic ratio versus the X-rays, electron and ion beam energy loss. Results indicate that a linear dependence on LET occurs, as will be presented and discussed.

1. Introduction

In radiation dosimetry it is important to consider the quantity of ionizing radiation absorbed in the target and the quality of radiation that induces specific effects, depending on the type of radiation and on the modality of its energy deposition [1]. The quantity of radiation is measured in terms of energy released to a unit of mass, i.e. in Gy = J/kg. The quality of radiation is measured by the Linear Energy Transfer (LET) of the radiation for unit of path in the target (keV/μm). Low LET radiations (electrons, γ and X-rays) generally produce less damage and disorder in the hit target with respect to high LET ones (α-particles and neutrons) [2].

The graphene oxide (GO) foils represent an innovative material constituted by 2D graphene sheets, with a size generally ranging between 0.1 and 10 μm, approximately parallel to each other, between which different oxygen functional groups are present [3–5]. These groups are mainly constituted by water molecules and hydroxyl (-OH), carboxyl (O═C–OH), carbonyl (C═O) and epoxide (C–O–C) groups chemically bonded to the sheet basal planes and edges [6].

The irradiation of GO by ionizing radiation induces chemical bonds breaking with elimination of water and oxygen functional groups, reducing the quantity of oxygen present in the carbon-based material and changing its chemical and physical properties [7]. The reduced graphene oxide (rGO) has high electrical and thermal conductivity, higher density, less crystalline order, high hydrophobicity, less roughness and other properties different with respect to the pristine GO, depending on the level of reduction, i.e. on the level of absorbed dose by the ionizing radiation [8,9].

Previous our papers show that the level of reduction, in GO 10-μm thick foils, grows with the absorbed dose displaying a linear increment at low doses (100 Gy-100 MGy) and a saturation at doses of the order of GGy or higher [10]. Such investigations have been performed with different radiations such as ions, electrons, laser beams and X and UV rays.

The GO foils, prepared in our laboratories [11], represent a type of dosimeter able to record the absorbed dose which can be maintained for long time, if the irradiated GO is conserved in vacuum or inert gas atmosphere at room temperature or at temperatures not higher than 50 °C [12]. The absorbed dose produces elimination of some oxygen functional groups, water and gas desorption, approach of the graphene

* Corresponding author. Dip.to di Scienze Fisiche, MIFT, Università di Messina, V.le F.S. D'Alcontres 31, 98166, Messina, Italy.
E-mail address: lorenzo.torrisi@unime.it (L. Torrisi).

https://doi.org/10.1016/j.vacuum.2022.111240
Received 9 May 2022; Received in revised form 6 June 2022; Accepted 7 June 2022
Available online 9 June 2022

micro-sheets, conductive carbon bridges between the sheets and greater compactness and density of the material [13].

Thus, realizing GO foils with thickness ranging from 10 to 100 μm by graphene oxide water dispersions, GO-based dosimeters with large or millimetric dimension, high flexibility and biocompatibility can be prepared at low cost and in a simple way. These so obtained dosimeters can be coated with a thin polymeric layer that can protect them from the absorption of gas and water vapor and that at the same time allows them to be exposed to penetrating radiations which, depositing their energy, produce removal of water and functional groups of oxygen from the graphene sheets. Sometimes the GO-based dosimeter can be used with the free surface without any coating film.

Research is in progress to realize more suitable dosimeters based on free GO, or on GO covered by polymer films or on GO composites according to both the type of radiation to be measured and the dosimetric aim.

For the reading of the absorbed dose different methods of analysis can be used, the choice of which depends on the sensitivity of the reduction level reading to be obtained. Simple dose readings can be obtained measuring the GO foils density, wetting ability, electrical conductivity and Fourier-transform infrared (FTIR) spectra, which depend on the absorbed dose. More sensitive methods can use the X-ray characteristic fluorescence emitted by carbon and oxygen and induced by (5–20) keV electron beams to measure the C/O atomic ratio using a Scanning Electron Microscope (SEM), or the X-rays diffraction produced, for example, by the K_α line of Cu (at about 8 keV). Even more sophisticated techniques, such as for example X-ray photoelectron spectroscopy (XPS), Auger electron spectroscopy, Elastic Recoil Detection Analysis (ERDA) and so on, can be employed to have a maximum information on the GO foil modifications induced by the absorbed dose.

The simple dose readings could be performed in simple laboratories, clinics and hospitals, while the more sophisticated ones could be carried out in highly equipped surface analysis laboratories.

In more detail, the dosimeter reading may be based on different analysis techniques, permitting the evaluation of the damage and of changes undergone by GO. The most used methods by us for the GO based dosimeter reading are the following:

i) the SEM/EDX (Electron dispersion X-ray) analysis induced by (5–30) keV electron beams to produce the characteristic X-ray fluorescence of the C- K_α line at about 287 eV and of the O- K_α line at about 525 eV. In this way it is possible to obtain a quick nondestructive determination of the elemental composition of the GO foil readily identifying carbon, oxygen and obtaining also morphological information. Furthermore, from the C and O X-ray yields, it is possible to evaluate the C/O atomic ratio, which is proportional to the absorbed dose [14];

ii) the μ-Raman spectroscopy using visible lasers to induce the characteristic vibrational peaks typical of the carbon-based materials: D (~1340 cm^{-1}), G (~1580 cm^{-1}) and 2D, D + G and C–H present in the (2600–3500) cm^{-1} region. In graphite the G peak is very sharp and located around 1060 cm^{-1} while the D peak gives information on the defects and damage to the structure. The A_D/A_G peaks area ratio grows linearly with the absorbed dose and can be considered an optimal dosimeter indicator. At high absorbed doses the D and G peaks blend and a new structure D" between G and D bands appears suggesting a higher disorder of the irradiated structure. Consequently, other Raman spectra parameters can be considered as dosimeter indicators, such as the G peak Full Width at Half Maximum (FWHM), the D" and the C–H peak areas [15];

iii) the Attenuated Total Reflection Fourier transform infrared spectroscopy (ATR-FTIR) performed in the wavenumber region (400–4000) cm^{-1} gives information on the different oxygen functional groups bonded to GO. In fact, measurements of transmittance or absorbance in this region, give indication on the amount of OH (~3030-3400 cm^{-1}), C–H (~2920 cm^{-1}), C═O (~1720 cm^{-1}), C═C (~1625 cm^{-1}), C–O (~1030-1150 cm^{-1} and 1400-1470 cm^{-1}) groups. Some of these groups are strongly present in the pristine GO and reduce proportionally to the absorbed dose, providing indication on both the level of reduction and the absorbed dose [16];

iv) X-ray photoelectron Spectroscopy (XPS) gives important information on the GO modifications induced by the radiation, evaluating qualitatively and quantitatively the different oxygen functional groups by the chemical shifts of the C1*s* and O1*s* XPS peaks and by their change in yield due to the absorbed dose. XPS can be employed for both analyzing and irradiating the GO foil thanks to its X-ray tube, as reported in the literature [17];

v) the X-ray diffractometry (XRD) equipped with a copper target, providing a Cu K_α radiation at about 8 keV energy, allows us to deduce the different levels of reduction in GO from the detailed analysis of the gathered XRD spectra. The pristine GO foil has a crystalline structure as results from the sharp diffraction peak at about 10.9° in 2θ. The reduction of GO with different techniques (thermal, laser and ionizing irradiations) induces damage and defects producing a disordered structure as suggested from the presence of only broad and weak features located at larger 2θ angles. These results indicate that rGO is more compact than the pristine GO and is more like graphene; at high doses, XRD spectra suggest the formation of new carbon phases, such as carbon nanotubes (CNT), amorphous carbon and others [15];

vi) the Selected Area Electron Diffraction (SAED) performed using the electron beam of a Transmission Electron Microscope (TEM) at the 80 keV energy has allowed us to acquire GO diffraction patterns showing distortion into its crystal structure due to the presence of defects in the graphene layers. The ionizing irradiations induce additional defects or remarkable damage into the GO crystal structure according to the prevalence of electronic or nuclear stopping power and there will be a progressive amorphization of the GO structure with the absorbed dose, as reported recently in one of our papers [18].

Of course many other methods of analysis of the GO foil - based dosimeters as a function of the absorbed dose can be employed with success, as presented in the literature, such as surface roughness, density, contact angle and wettability, electrical conductivity measurements, Auger spectroscopy, neutron diffraction, Rutherford backscattering spectrometry (RBS), ERDA, optical spectroscopy and others [8,18–20].

The GO-based dosimeters compared to the traditional polymeric CR39 track detectors or to the GAF-chromic films [21,22] are readable with a simple method of analysis, reproducible, flexible, biocompatible, cheap, they can be millimetric in size and more sensitive to the level of absorbed dose. However, their main disadvantage is being partially altered by the long permanence in air or higher temperatures than 50 °C; consequently, they should be saved in vacuum or in inert environment. Of course, to be able to consider the GO-based dosimeters reliable for radioprotection and clinical dosimetry they still need to be subjected to a more detailed study with different radiations.

Regardless of how the GO dosimeter reading is done we must remember that the effects induced in the pristine GO structure by low, medium and high LET radiation are different. In fact, the low LET radiation gives rise to mainly electronic energy release with production of ionizations and partial chemical bond ruptures; the medium LET radiation induces electronic and partially nuclear energy release with high level of ionizations, chemical bonding rupture, radical and new molecules formation; the high LET radiation causes a high nuclear energy release with consequent atomic collisions and atoms displacements, chemical bond breaking and high degrees of carbon amorphization [23].

In this paper, the main aim is to investigate the LET dependence of the effects induced by different incident radiations in the pristine GO to

establish if the GO-based dosimeter is dependent on LET or not. To attain this, different results of the GO reduction induced by soft X-rays, electron beams and low and high energy ion beams will be presented and discussed.

2. Materials and methods

2.1. Photon beams

XPS analysis has been carried out using a VG Scientific ESCALab Mk II twin-anode XPS spectrometer operating in ultra-high vacuum (of the order of 10^{-9} mbar), at an anodic voltage of 10 kV in the constant pass-energy mode at 20 eV with an energy resolution (FWHM) of 1.0 eV as detected by the Ag $3d_{5/2}$ emission. The soft X-photon beam is not monochromatic and is produced by a twin anodes VG XR2 X-ray source, equipped with an Al anode working at a 32 mA emission current and at 320 W power. This soft X-ray beam has an energy of about 1486.6 eV. The calibration and linearity of the binding energy scale has been confirmed by measuring the positions of Au $4f_{7/2}$, Cu $2p_{3/2}$, and Ag $3d_{5/2}$ core-level peaks from uncontaminated metal standard stubs. The GO sample was approximately 3.6 cm distant from the Al anode and separated from it by a 2 μm Al foil window, that shows a transmittance at 1486.6eV of about 80.7%, as calculated by the CXRO code [24]. The Al window at the X-ray tube output has a diameter of about 7 mm and it is about 6 mm distant from the anode, thus the X-rays solid emission angle is about 1.069 sr. Therefore, the soft X-ray beam spot size at 3.6 cm from the Al anode is of about 4.2 cm in diameter. Since the GO foils have a circular shape with an about (6 ÷ 11) mm diameter and are centered in the XPS stub, they are completely irradiated by the X-rays beam. The base pressure during spectra acquisition is better than $3x10^{-8}$ mbar and is achieved by an ion pump system supplied with the spectrometer. The Al-K_α photon flux on the GO foil is of about $2.25x10^{12}$ photons/cm^{2}s. A single XPS scan lasts just over 5 min, an acquisition time that has allowed to obtain a good statistics XPS spectrum. More details are given in Ref. [17]. High-resolution XPS spectra relative to the C1s and O1s core level regions have been collected sequentially at an about 45° emission angle. Owing to the sample charging, the first component of the C1s spectra, due to the C–C/C═C bonds from GO, was fixed to 285.0 eV as reported in the literature [25], assuming that the contribution of adventitious carbon is negligible. In our opinion, this is the only method to correct the XPS spectra obtained from the poorly conducting samples which contain C–C/C═C bonds as an inherent part of the specimen (in contrast to C–C/C═C bonds from adsorbed adventitious carbon layer) as is the case with graphene oxide [9]. For samples that exhibit a good electrical conductivity, on the other hand, a new approach, based on a complementary measurement of the sample work function, is recently reported in the literature [26,27] that, as indicated by the same authors, is not expected to work properly for poorly conducting samples such as GO. By changing the irradiation time, between about 5 min and 450 min, it has been possible to irradiate the GO samples in ultra-high vacuum with different doses. The level of reduction in the X-ray irradiated GO samples has been measured using XPS.

2.2. Electron beams

Electron beams at the (5–10) kV energies have been produced by a Zeiss SEM microscope (model Crossbeam 540) equipped with an EDX micro-probe. The electron beam hits sample areas of the order of 100 μm × 50 μm with currents in the (400–800) pA range. The EDX probe permits the detection of the C and O K_α characteristic X-ray lines, respectively at about 287 eV and 525 eV. Each X-ray spectrum has been acquired in times of (10–100) s, while the electron beam irradiation has been performed in times from 10 s up to 1000 s and more. The SEM-EDX software, considering the detection efficiency of the EDX system, the X-ray production cross-section at the electron beam energy, the used beam-detector geometry and the electron incidence angle, gives the atomic composition of the investigated material, from which it is possible to deduce the C/O atomic ratio [28]. The electron energy deposition, the range, the straggling and the electron backscattering in GO have been calculated using the SREM code [29]. The level of reduction in the electron irradiated GO targets has been measured using EDX.

2.3. Ion beams

Ion beams accelerated using the 3 MV Tandetron of NPI-ASCR in the Czech Republic have

been employed to irradiate the 10 μm thick GO foils in high vacuum. H^+, He^+, O^{5+}, Cu^{5+}, Au^{5+} are some of the used ion beams at energies between 1 MeV and 16 MeV depositing energy in the GO target via electronic and nuclear interactions. Generally, the ion beam current density is maintained at values of about 0.5 μA/cm^2 and the spot is of about 1 cm^2. Fluence has been varied between about 10^{13} and 10^{16} ions/cm^2, corresponding to absorbed doses ranging between about 100 Gy and 100 MGy. In the 10 μm thick GO foils some ion beams are transmitted, and others are full stopped. The ion range, stopping power, straggling and electronic and nuclear ion energy deposition have been calculated using the SRIM code [30]. The measured density of pristine GO is of about 1.36 g/cm^3, while that of rGO ranging from 1.5 to 1.9 g/cm^3 depending on level of reduction. The level of reduction in the ion beam irradiated GO foils has been measured using XPS, EDX, Raman spectroscopy, X-ray diffraction analysis, and electrical conductivity measurements, as reported in our previous papers [15,17,31,32].

3. Results and discussion

3.1. XPS spectroscopy

Using the Al K_α soft X photon flux value $\varphi = 2.25\ x10^{12}$ photons/cm^{2}s and the investigated irradiation times Δt and assuming the photon spot S = 1 cm^2, it has been possible to calculate the absorbed dose D_a (Gy) in the irradiated GO samples. Remembering that the soft X photon (Al K_α line) energy can be approximated to $E_f = 1487$ eV, one can calculate, by employing the CXRO code, the absorption A at the analysed GO depth of 5 nm obtaining $A = 5.4x10^{-4}$. Thus, this photon flux for 1 s irradiation time (Δt) and 1 cm^2 surface (S) corresponds to an energy deposition rate ΔE of:

$$\Delta E_{Al\text{-}K\alpha} = E_f \varphi A S \Delta t = (1487x1.6x10^{-19}J)(2.25x10^{12}ph/cm^2s)(5.4x10^{-4})(1\ cm^2)(1s) = 2.89x10^{-7}J/s \quad (1)$$

Considering that the analysed XPS thickness (Δz) is of about 5 nm and assuming that the ρ density of the irradiated GO surface is of about 1.5 g/cm^3, the irradiated GO mass M is:

$$M = \rho\ S\ \Delta\ z = (1.5\ g/cm^3)\ (1\ cm^2)\ (5x10^{-7}\ cm) = 7.5x10^{-7}g = 7.5x10^{-10}\ kg \quad (2)$$

Consequently, the absorbed dose-rate D_r, in Gy/s units, is given by:

$$D_r\ (Al\text{-}K_\alpha\ line) = \Delta E_{Al\text{-}K\alpha}\ (J/s)\ /\ M\ (kg) = 385\ Gy/s \quad (3)$$

Such dose-rate values are comparable to those reported in the literature for similar soft X-ray irradiations of GO sample [16].

XPS is a very interesting technique for the materials characterization from the composition and bonds point of view because the binding energy of a chemical element is a function of the chemical environment in which it is located. It measures the so-called chemical shifts, which are function of the type of bond shared with other chemical elements.

Fig. 1 shows the high-resolution C1s (on the left) and O1s (on the right) core level regions XPS spectra after the exposure to the 1486.6 eV Al K_α radiation. The pristine GO foil, after 12 min of soft-X ray irradiation corresponding to an about 276 kGy dose (see Fig. 1a), shows a C1s XPS spectrum made up of two large peaks at about 285.6 eV and 288.4

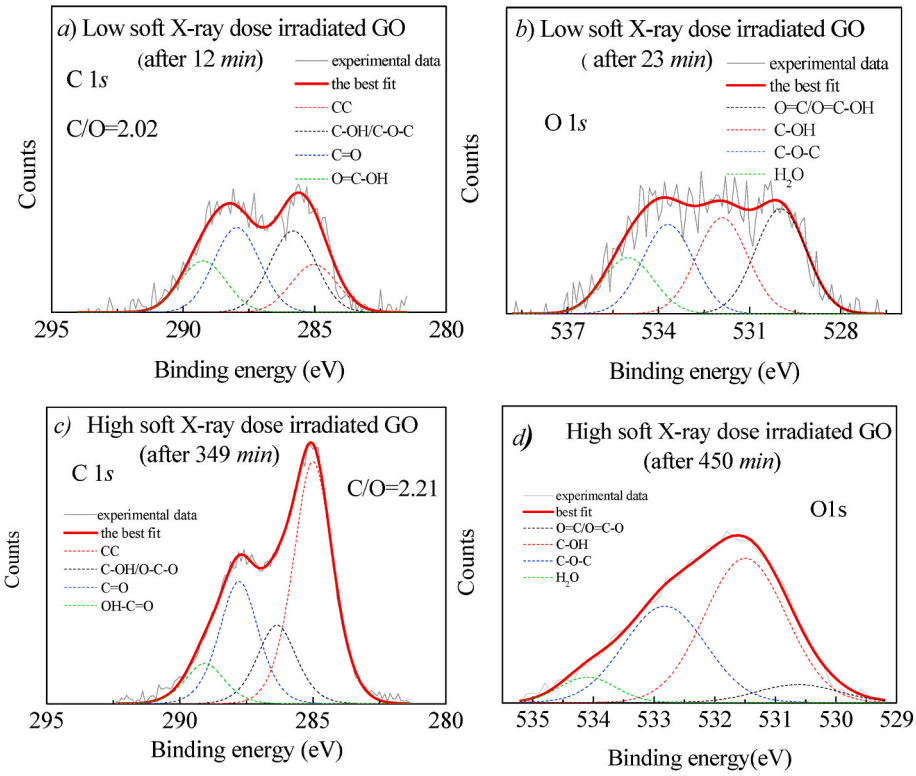

Fig. 1. High resolution XPS spectra of the C 1s (on the left) and O 1s (on the right) core level regions for soft X-ray absorbed dose at low (a, b) and high level (c, d).

eV that can be fitted to sub-bands at about 285.0, 285.8, 288.0 and 289.2 eV.

These structures can be assigned respectively to C–C and C═C, C–O (in epoxy and hydroxyl groups), C═O (in carbonyl groups) and O═C–OH (in carboxylic groups). In the following, CC refers to the sum of the C–C and C═C bonds, while CO designates all the combinations of links between the C and O atoms [17].

When GO is soft X-ray irradiated for longer times, the ratio of the different sub-bands is modified, and one can assume the irradiation time as representative of the GO absorbed dose. For the longest soft X-ray irradiation time, corresponding to 349 min for C1s and to an 8020 kGy absorbed dose, as shown in Fig. 1c, the 285.0 eV sub-band, due to the C–C and C═C links, increases in intensity, while the other ones, attributed to the C–OH/C–O–C, C═O and O═C–OH functional groups decrease, in agreement with the literature [9].

This result suggests an increasing partial removal of oxygen-containing functional groups with the irradiation time as also indicated by the slight increment of the C/O ratio and, therefore, a partial reduction of GO in good agreement with the literature [9,17].

With respect to the high-resolution O1s XPS spectrum, it is also strongly modified by the soft X-rays irradiation for times going from 23 min to 450 min corresponding respectively to about 529 kGy and 10340 kGy doses, as one can see in Fig.s 1b and 1d. In particular, the C═O/O═C–OH and H_2O sub-bands area decreases, while the C–OH and C–O–C components increase and the C–OH one prevails according to the literature [17]. Thus, increasing the soft X-ray irradiation time or the soft X-rays absorbed dose, GO reduces itself due to the continuous decrease on the oxygen containing functional groups.

Fig. 2 shows the CC/CO ratio between the chemically carbon-carbon bonds with respect to the carbon-oxygen links in the C1s peak, as a function of both the irradiation time and the soft X-rays dose. This parameter, as the plot indicates, is linearly proportional to the soft X-ray absorbed dose in the (276 kGy- 8.0 MGy) investigated range.

No limitation and no saturation level occur at low and high doses. By considering the XPS spectra reproducibility and the counting statistics, it has been evaluated that the experimental data, also reported in Table 1, are affected by an error of about 3% for the XPS yield.

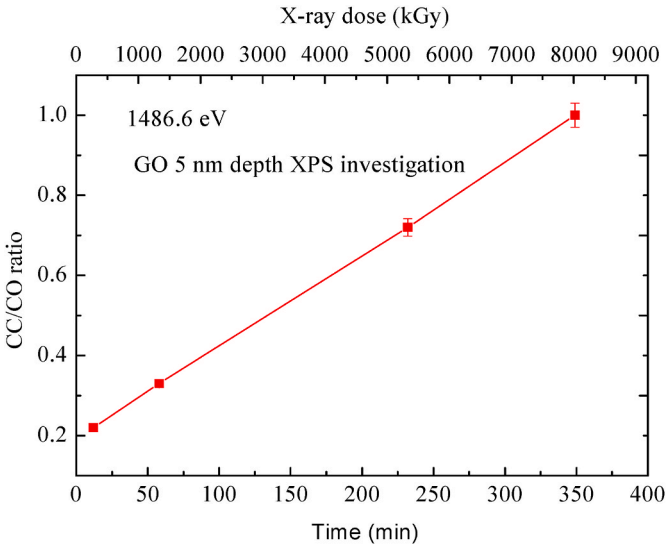

Fig. 2. XPS yield, in terms of the CC/CO ratio in the C1s core level region, as a function of the irradiation time and of the soft X-rays absorbed dose.

This CC/CO-dose response curve suggests the possibility to realize a dosimeter with these thin GO foils.

3.2. EDX spectroscopy

In the case of electron beam irradiation, the electron energy is 5 keV at which corresponds a SREM calculated electron range in GO (1.5 g/cm^3) of about 350 nm. In this case, the GO reduction can be measured through the EDX analysis, performed through the SEM probe, by

Table 1
CC/CO and C/O ratios calculated by XPS vs soft X-ray irradiation time and absorbed dose.

$t_{\text{soft X-ray irradiation exposure}}$ (min)	CC/CO	X-ray dose (kGy)	C/O
12	0.22	275.76	
23		528.54	2.02
46		1060	2.03
58	0.33	1330	
220		5060	2.18
232	0.72	5330	
349	1.00	8020	
450		10340	2.21

evaluating the yield of the C and O K_α characteristic X-ray fluorescence lines at about 287 eV and 525 eV respectively, and by calculating the C/O atomic ratio. Fig. 3 shows the EDX spectra of the pristine GO and of the 5 keV electron irradiated GO after different absorbed doses, as presented in similar investigation reported in the literature [10]. Increasing the electron absorbed dose the reduction level increases, some functional oxygen groups and water desorb in vacuum, and the EDX measured C/O atomic ratio increases. The EDX analysis is referred to the surface layers from which C and O characteristic X-rays come out, which correspond to about one half of the electron range in GO. Thus, considering the electron beam energy $E_0 = 5$ keV, the electron beam current I = 400 pA, the irradiated spot S of 300 μm × 300 μm = $9x10^{-4}$ cm^2 and the electron charge *e*, the deposited energy into the 350 nm irradiated depth for the Δt = 1 s irradiation time is:

$$\Delta E(\text{electrons}) = (E_0 I \cdot S \cdot \Delta t)/(S \cdot e) = (5x10^3 x 1.6x10^{-19} J \times 400 \times 10^{-12} \text{ C/s x } 1s)/(1.6x10^{-19} \text{ C}) = 2 \text{ μJ} \quad (4)$$

The irradiated mass is:

$$M = \rho \, S \, \Delta z = (1.5 \text{ g/cm}^3)(9x10^{-4} \text{cm}^2)(350x10^{-7} \text{ cm}) = 47.25x10^{-9} \text{ g} = 47.25x10^{-12} \text{ kg} \quad (5)$$

Consequently, the absorbed dose-rate D_r, in Gy/s units, is given by:

$$D_r \text{ (electrons)} = \Delta E(\text{electrons}) \text{ (J/s)} / M \text{ (kg)} = (2 \text{ μJ/s})/47.25x10^{-12} \text{ kg} = 42 \text{ kGy/s} \quad (6)$$

Thus, the EDX spectra shown in Fig. 3 and the given C/O atomic ratios are referred to an absorbed electron dose of about 3.72 MGy (Fig. 3a), 150 MGy (Fig. 3b), 550 MGy (Fig. 3c) and 5000 MGy (Fig. 3d) respectively.

Plotting the so deduced C/O atomic ratio values versus the electron absorbed dose a linear growth with the dose is observed at low absorbed dose, while at high absorbed dose a saturation trend is visible as one can see Fig. 4. At doses of the order of tens GGy, the C/O ratio in vacuum saturates to a value of about 4.6.

This C/O-dose response curve confirms the previously suggested possibility to realize a dosimeter with these thin GO foils. By considering the EDX spectra reproducibility and the counting statistics, it has been evaluated that the experimental data, also reported in Table 2, are

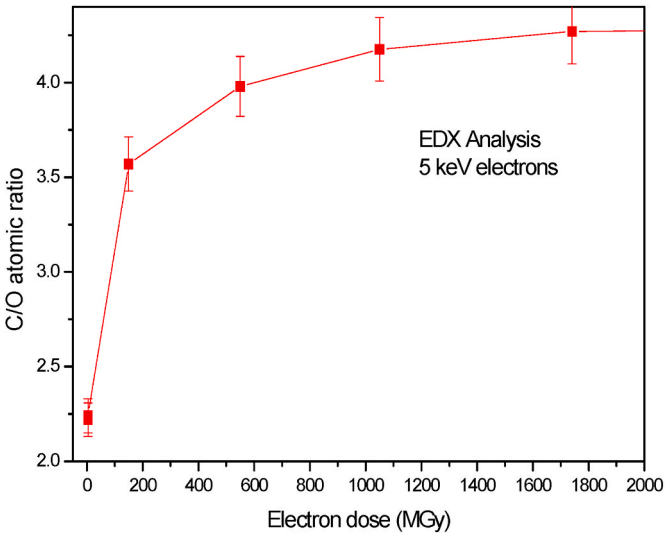

Fig. 4. C/O atomic ratio from EDX analysis versus electron absorbed dose.

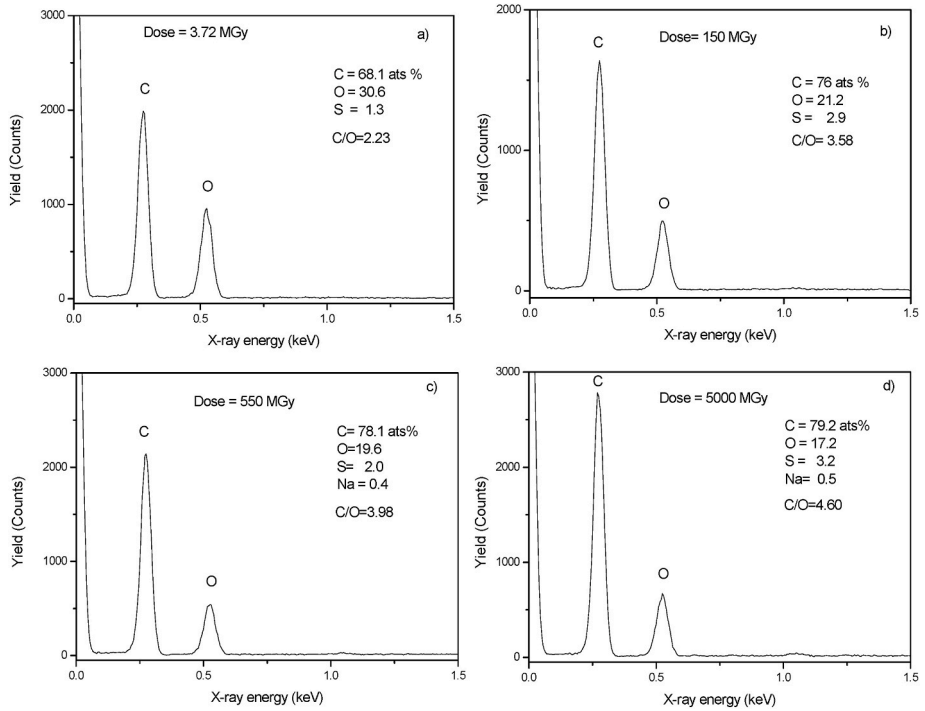

Fig. 3. EDX analysis of the GO foils at different absorbed electron doses.

Table 2
Electron irradiation time, electron dose and C/O atomic ratio measured using SEM/EDX analysis.

electron irradiation exposure Δt (s)	Electron dose (MGy)	C/O atomic ratio
100	4.2	2.24
357	15	3.57
2500	1050	4.20
4150	1743	4.6

affected by an error of about 4% for the characteristic X-ray yields.

3.3. Ion beam irradiation

Ion beams at different energy and stopping power have been employed in this experiment to irradiate GO foils with 10 μm thickness in high vacuum (10^{-6} mbar). The used beams have been H^+, He^+, $O^{4,5+}$, Cu^{5+} and Au^{5+} with energy and fluence ranging between 2 MeV and 16 MeV and between about $5x10^9$ ions/cm^2 and $5x10^{15}$ ions/cm^2, respectively. To evaluate the level of reduction induced by the ion irradiation, the irradiated targets have been investigated in different ways, using EDX analysis, XPS and Raman spectroscopies and XRD. Fig. 5 reports the EDX C/O atomic ratio variation as a function of the ion fluence for the different used ion types.

The trend is linear with the fluence for low stopping power ions, such as protons and helium, while it is over-linear for high stopping power ions, such as copper and gold. The C/O variation indicates that the reduction level grows using heavy ions, and that in this case a saturation trend will be observed at higher fluences than the investigated ones.

The absorbed ion dose by the irradiated GO foil has been calculated using the ion fluence F (ions/cm^2), the ion energy loss in the sample ΔE/Δx (keV/μm), and the mass of the irradiated material. This last has been evaluated by the irradiated volume, given by the S ion beam spot size, the Δx ion range and the GO density ρ. Since the EDX analysis is performed in the first micron of surface, depending on the electron range, the absorbed dose D_a, in Gy, has been calculated in the first layers using the equation:

$$D_a = F \cdot \left(\frac{\Delta E}{\Delta x}\right) \cdot \left(\frac{1}{\rho}\right) (Gy) \quad (7)$$

The C/O atomic ratio depends on the type of ion beam, i.e. on the stopping power of the ion in GO. Lower stopping power ions, such as proton and helium, show low levels of reduction, while high stopping power ions, such as copper and gold, show high C/O atomic ratio indicating high level of reduction induced in the irradiated structure. The C/O ratio depends linearly on the absorbed dose for doses lower than about 500 MGy, while it tends towards a saturation value for higher doses, as reported in the literature [10]. Fig. 6 displays the measured EDX C/O atomic ratio as a function of the ion dose for the different ions. The result demonstrates that at the same absorbed dose, the C/O atomic ratio is different for the different ion species, increasing with the ion mass and stopping power. Thus, the GO reduction level is not a simple linear function of the absorbed dose, but it depends on many other parameters, such as the ion species and the ion stopping power.

Table 3, for example, shows the different C/O atomic ratios measured for proton beams and copper ion beams as a function of the ion energy and stopping power. The proton beams release electronic energy along their ion path, with generation of ionization, deexcitations, molecular scissions and radical formation, increasing slightly the C/O atomic ratio for the low level of reduction induced in GO. The copper ion beams lose energy due to electronic and nuclear interactions, generating atom collisions and dislocations, breaking many molecular bonds, especially in the ion range, increasing significantly the C/O atomic ratio and inducing high level of reduction in GO [10].

3.4. Level of GO reduction versus LET

The different EDX C/O atom ratio evaluations have been carried out to measure the level of GO reduction due to its irradiation with soft X-rays, keV electrons and MeV ion beams. This has allowed us to analyze the obtained level of reduction as a function of the Linear Energy Transfer (LET) of different ionizing radiations. Fixing the absorbed dose with X-rays, electrons and ions to 10 MGy and 100 MGy, we have evaluated their level of reduction from the EDX C/O atomic ratio and plotted this parameter as a function of the radiation LET, in keV/microns units, as shown in Figs. 7 and 8, respectively. The measurements error is of about 4%.

To calculate the corresponding LET, a GO foil, 1 μm thick, with a C/O value, without any absorbed dose, of 1.435 and a density of 1.5 g/cm^3, has been used. A fast 1.49 eV soft X-ray irradiation has been performed on GO in vacuum. Being the Al K_α X-ray in this GO foil, calculated with the CXRO code about 90%, an X-ray LET of about 0.15 keV/μm is derived. A fast electron irradiation with a10 keV electron beam has been performed and an electronic energy loss in GO of about 7.14 keV/μm has been evaluated by the SREM code. For protons, having high electronic energy deposition and for heavy ions, having high nuclear energy

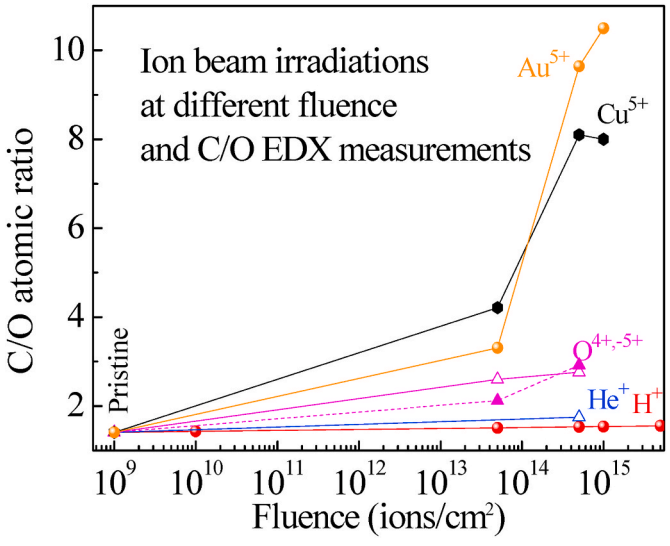

Fig. 5. EDX C/O atomic ratio versus ion fluence for different ion beams (H^+, He^+, O^{4+}, O^{5+}, Cu^{5+} and Au^{5+}).

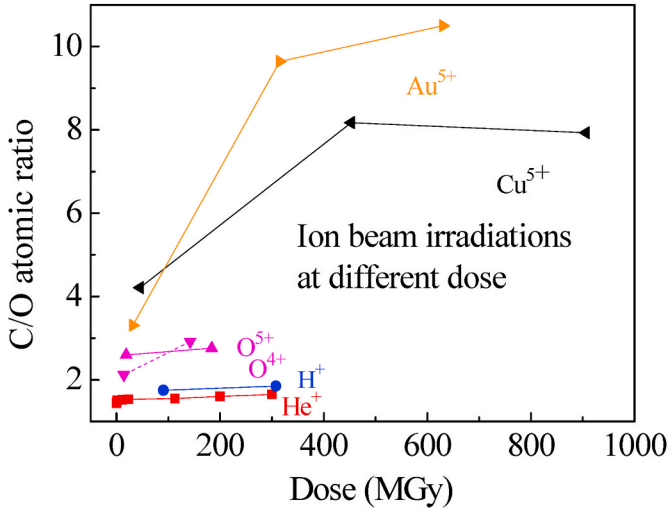

Fig. 6. EDX C/O atomic ratio versus the absorbed ion dose for different ion beams (H^+, He^+, O^{4+}, O^{5+}, Cu^{5+} and Au^{5+}).

Table 3
C/O atomic ratio for proton and copper ion beams at different energy, fluence and absorbed dose.

Ion beam	Energy (MeV)	Electronic energy loss (keV/μm)	Nuclear energy loss (keV/μm)	Total energy loss (keV/μm)	Fluence (ions/cm^2)	Absorbed dose (MGy)	C/O
Protons	2.0	24.1	0.014	24.1	5x10^{13}	1.13	1.51
"	"	"	"	"	5x10^{14}	11.3	1.52
"	"	"	"	"	1x10^{15}	22.6	1.53
"	"	"	"	"	5x10^{15}	113	1.55
Copper	16	4758	54.2	4812.2	5x10^{13}	45.3	4.2
"	"	"	"	"	5x10^{14}	453	8.0
"	"	"	"	"	1x10^{15}	906	7.8
Pristine GO						0	1.435

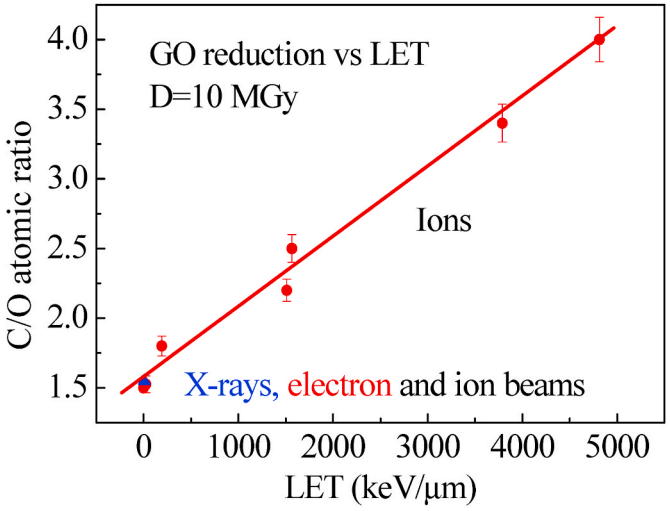

Fig. 7. EDX C/O atomic ratio versus the radiation LET for an absorbed dose of 10 MGy.

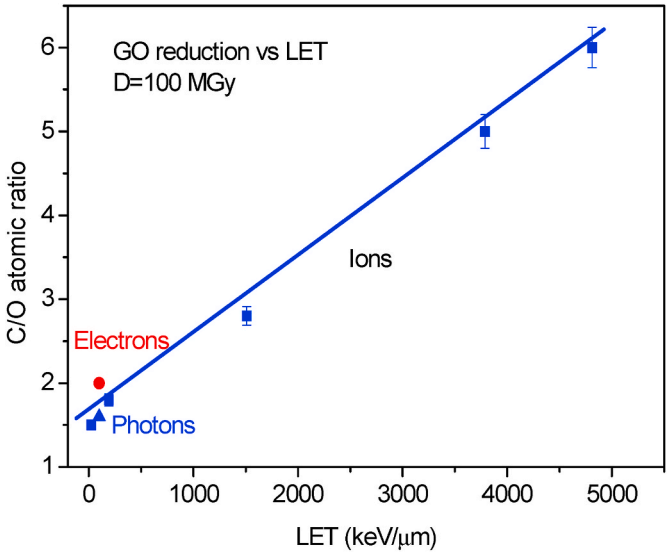

Fig. 8. EDX C/O atomic ratio versus the radiation LET for an absorbed dose of 100 MGy.

deposition, the energy loss has been calculated at the different ion species and energy using the SRIM simulation code.

The GO reduction dependence on the LET increases for high LET radiations, such as heavy ions at high and low energy, which induce high deoxygenation with damage to the layered structures of the GO foil, as demonstrated by the Raman spectroscopy and X-ray and electron beam diffraction in previous our papers [15,33].

Fig. 9 reports the comparison of the C/O atomic ratio as a function of the radiation LET for three different levels of absorbed dose: 10 MGy, 100 MGy and 300 MGy. Thus, GO foils can be used as dosimeters for their good proportionality of the reduction level with the absorbed dose, but it is necessary to remember that their response is not independent on the radiation LET, but it linearly depends on LET. Low LET radiation and small doses induce low level of reduction, as occurs for photons, electrons and high energy proton beams. On the contrary, high LET radiation and large doses produce high level of reduction and permanent damage in the irradiated GO, as happens for heavy ions and low energy sputtering ions. The here reported our evaluation has been based on the C/O atomic ratio vs LET, but similar deductions can be obtained considering other types of "reading" of the dosimeter, i.e. using Raman spectroscopy, XRD, electrical conductivity and so on.

4. Conclusions

This paper deals with a low cost and easy preparation method of GO foils consisting in depositing on a suitable substrate a water dispersion containing 4 wt% graphene oxide micrometric sheets. The so obtained GO foils with thickness of 10 μm can be used as dosimeters with millimetric-centimetric surface size thanks to the material reduction by absorption of ionizing radiations.

Soft X-rays, electron and ion beams have been tested to induce in vacuum the GO reduction that has been evaluated from different types of analysis. Characteristic X-ray fluorescence (EDX) and X-ray photoelectron spectroscopy (XPS) have been employed in this paper because they give proportional information to the level of reduction and to the absorbed dose by the GO foil.

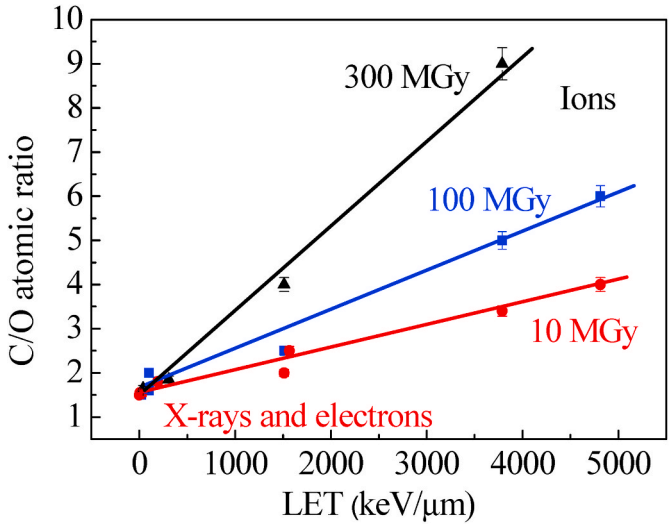

Fig. 9. C/O atomic ratio versus the radiation LET for three different absorbed doses: 10, 100 and 300 MGy.

An important not solved dosimetric question concerns the independence or dependence on the radiation LET of the realized dosimeter. To answer this, the measurement presented in this paper have been performed by using radiations at low and high LET and the EDX atomic C/O ratio. Its increment with the reduction level induced by the irradiation is linear with LET and rises with the absorbed doses. At low LET and small absorbed doses the level of reduction remains low, while at high LET and great absorbed dose it is significant. In this last case the high measured values of C/O ratios and the different analyses of the irradiated GO foils demonstrate that a permanent foil damage is produced.

Although different analysis techniques can be employed to measure the reduction level in the GO-based dosimeter, in clinical and hospital environment its readout could require a simple apparatus such as a SEM/EDX system. For research activity in highly specialized laboratories more sophisticated and expensive techniques (such as XPS and μRaman spectroscopies, XRD, …) could be used.

CRediT authorship contribution statement

L. Torrisi: Writing – original draft. **L. Silipigni:** Investigation. **M. Cutroneo:** Investigation. **E. Proverbio:** Investigation. **A. Torrisi:** Investigation.

Declaration of competing interest

The authors declare that they have no known competing financial interests or personal relationships that could have appeared to influence the work reported in this paper.

Data availability

Data will be made available on request.

Acknowledgements

Authors thank the INFN for the useful support given to this research through the CIMA project.

Many thanks also to the CANAM Laboratory of the ASCR in Rez, Czech Republic, for the useful support given, irradiating the samples with different ion beams. Supported by OP RDE, MEYS, Czech Republic under the project CANAM OP, CZ.02.1.01/0.0/0.0/16_013/0001812 and by the Czech Science Foundation (GACR No. 22-10536S).

References

[1] K.R. Kase, B.E. Biarngard, F.H. Attix, The Dosimetry of Ionizing Radiation, V. I & V. II, Academic Press Inc., New York, 1985.
[2] M. Scholz, Microdosimetric response of physical and biological systems to low- and high-LET radiations, cap. I, in: Y. Horowitz (Ed.), Theory and Applications to Dosimetry", vols. 1–73, Elsevier, 2006, ISBN 978-0-444-51643-5.
[3] M. Aliofkhazraei, N. Ali, W.I. Milne, C.S. Ozkan, S. Mitura, J.L. Gervasoni (Eds.), Graphene Science Handbook, Mechanical and Chemical Properties, C*RC Press*, Taylor & Francis Group, Boca Raton, 2016.
[4] M. Aliofkhazraei, N. Ali, W.I. Milne, C.S. Ozkan, S. Mitura, J.L. Gervasoni (Eds.), Graphene Science Handbook, Electrical and Optical Properties, *CRC Press*, Taylor & Francis Group, Boca Raton, 2016.
[5] K.S. Vasu, R. Krishnaswamy, S. Sampathc, A.K. Sood, Yield stress, thixotropy and shear banding in a dilute aqueous suspension of few layer graphene oxide platelets, Soft Matter 9 (2013) 5874.
[6] N.S. Suhaimin, M.F.R. Hanifah, J.W. Jusin, J. Jaafar, M. Aziz, A.F. Ismail, M.H. D. Othman, M.A. Rahman, F. Aziz, N. Yusof, R. Mohamud, Tuning the oxygen functional groups in graphene oxide nanosheets by optimizing the oxidation Time, Phys. E Low-dimens. Syst. Nanostruct. 131 (2021), 114727.
[7] F. Xu, R. Chen, Z. Lin, X. Sun, S. Wang, W. Yin, Q. Peng, Y. Li, X. He, Variable densification of reduced graphene oxide foam into multifunctional high-performance graphene paper, J. Mater. Chem. C 6 (2018), 12321.
[8] L. Torrisi, M. Cutroneo, A. Torrisi, L. Silipigni, Measurements on five characterizing properties of graphene oxide and reduced graphene oxide foils, 2100628, Phys. Solid State (2022) 1–9.
[9] L. Silipigni, G. Salvato, G. Di Marco, B. Fazio, A. Torrisi, M. Cutroneo, L. Torrisi, Band-like transport in high vacuum thermal reduced graphene oxide films, Vacuum 165 (2019) 254–261.
[10] L. Torrisi, L. Silipigni, D. Manno, A. Serra, V. Nassisi, M. Cutroneo, A. Torrisi, Investigations on graphene oxide for ion beam dosimetry applications, Vacuum 178 (2020), 109451.
[11] L. Torrisi, M. Cutroneo, V. Havranek, L. Silipigni, B. Fazio, M. Fazio, G. Di Marco, A. Stassi, A. Torrisi, Self-supporting graphene oxide films preparation and characterization methods, Vacuum 160 (2019) 1–11.
[12] B. Lian, S. De Luca, Y. You, S. Alwarappan, M. Yoshimura, V. Sahajwalla, S. C. Smith, G. Leslie, R.K. Joshi, Extraordinary water adsorption characteristics of graphene oxide, Chem. Sci. 9 (2018) 5106–5111.
[13] D. Yang, A. Velamakanni, G. Bozoklu, S. Park, M. Stoller, R.D. Piner, S. Stankovich, I. Jung, D.A. Field, C.A. Ventrice, R.S. Ruoff, Chemical analysis of graphene oxide films after heat and chemical treatments by X-ray Photoelectron and Micro-Raman spectroscopy, Carbon 47 (2009) 145–152.
[14] L. Torrisi, L. Silipigni, M. Cutroneo, Radiation effects of IR laser on graphene oxide irradiated in vacuum and in air, Vacuum 153 (2018) 122–131.
[15] D. Manno, A. Serra, A. Buccolieri, L. Calcagnile, M. Cutroneo, A. Torrisi, L. Silipigni, L. Torrisi, Structural and spectroscopic investigations on graphene oxide foils irradiated by ion beamsfor dosimetry application, Vacuum 188 (2021), 110185.
[16] A.F. Madsuha, M.S. Wahab, S. Daulay, E.S. Rosa, D. Dhaneswara, A. H, Yuwono integration of reduced graphene oxide in platinum-free counter electrode of dye-sensitized solar cell, Mater. Sci. Forum 1000 (2020) 12–19.
[17] L. Torrisi, L. Silipigni, M. Cutroneo, A. Torrisi, Graphene oxide as a radiation sensitive material for XPS dosimetry, 109175, Vacuum 173 (2020) 1–8.
[18] D. Manno, L. Torrisi, L. Silipigni, A. Buccolieri, M. Cutroneo, A. Torrisi, L. Calcagnile, A. Serra, From GO to rGO: an analysis of the progressive rippling induced by energetic ion Irradiation, Appl. Surf. Sci. 586 (2022), 152789.
[19] M. Cutroneo, V. Havranek, A. Mackova, P. Malinsky, L. Torrisi, L. Silipigni, B. Fazio, A. Torrisi, K. Szokolova, Z. Sofer, J. Stammers, Effects of the ion bombardment on the structure and composition of GO and rGO foils, Mater. Chem. Phys. 232 (2019) 272–277.
[20] H.A. Becerril, J. Mao, Z. Liu, R.M. Stoltenberg, Z. Bao, Y. Chen, Evaluation of solution-processed reduced graphene oxide films as transparent conductors, ACS Nano 2 (3) (2008) 463–470.
[21] E.E. Kading, O. Aviv, I. Eliyahu, M. Gai, S. Halfon, M. Hass, C.R. Howell, D. Kijel, Y. Mishnayot, I. Mukul, A. Perry, Y. Shachar, Ch Seiffert, A. Shor, I. Silverman, S. R. Stern, Th Stora, D.R. Ticehurst, A. Weiss, L. Weissman, Tests and calibrations of nuclear track detectors (CR39) for operation in high neutron flux, Physical Rev. Research 2 (2020), 023279.
[22] Ashland GAFCHROMIC EBT, Garchromic EBT Films - GAFchromic™, 2022 actua website.
[23] E.L. Alpen, Quantities, units, and definitions, cap, in: Radiation Biophysics, second ed. vol. 1, Academic Press, Elsevier, 1998, pp. 1–10.
[24] CXRO, X-Ray Interactions with Matter, Actual Website, 2022. Filter Transmission (lbl.gov).
[25] G. Sobon, J. Sotor, J. Jagiello, R. Kozinski, M. Zdrojek, M. Holdynski, P. Paletko, J. Boguslawski, L. Lipinska, K.M. Abramski, Graphene Oxide vs. Reduced Graphene Oxide as saturable absorbers for Er-doped passively mode- locked fiber laser, Opt Express 20 (17) (2012), 19463.
[26] G. Greczynski, L. Hultman, Reliable determination of chemical state in x-ray photoelectron spectroscopy based on sample- work-function referencing to adventitious carbon: resolving the myth of apparent constant binding energy of the C1s peak, Appl. Surf. Sci. 451 (2018) 99.
[27] G. Greczynski, L. Hultman, X-ray photoelectron spectroscopy: towards reliable binding energy referencing, Prog. Mater. Sci. 107 (2020), 100591.
[28] N. Bano, I.H. Asghar, A. El-Naggar, A.A. Albassam, Reduced graphene oxide nanocomposites for optoelectronics applications, Appl. Phys. A 125 (3) (2019) 125–215.
[29] SREM, The Stopping and Range of Electrons in Matter, actual website, 2022. SREM (srim.org).
[30] J. Ziegler, M. Ziegler, J. Biersack, SRIM – the stopping and range of ions in matter, 2008, Nucl. Instrum. Methods B 268 (2010) 1818–1823.
[31] M. Cutroneo, L. Torrisi, J. Badziak, M. Rosinski, A. Torrisi, M. Fazio, Z. Sofer, R. Bottger, S. Akhmadaliev, Hybrid graphene-based material promising target in laser matter interaction, C011021, J. Inst. Met. 15 (1) (2020) 1–13.
[32] P. Malinskýa, M. Cutroneo, V. Hnatowicz, J. Stammers, J. Luxa, K. Szőkölová, Z. Sofer, A. Macková, Study of supported CVD graphene irradiated by He and Au ions, Vacuum 170 (2019), 108952.
[33] K. Saravanan, G. Jayalakshmi, K. Suresh, B. Sundaravel, B.K. Panigrahi, D. M. Phase, Structural evaluation of reduced graphene oxide in graphene oxide during ion irradiation: X- ray absorption spectroscopy and in-situ sheet resistance studies, Appl. Phys. Lett. 112 (2018), 111907.